WIND TUNNEL TESTS OF FOUR FLEXIBLE
WING ULTRALIGHT GLIDERS

Robert A. Ormiston
Aeromechanics Laboratory
US Army Research and Technology Laboratories (AVRADCOM)
Moffett Field, Calif. 94035

SUMMARY

The aerodynamic lift, drag, and pitching moment characteristics of four
full scale, flexible wing, ultralight gliders were measured in the
settling chamber of a low speed wind tunnel. The gliders were tested
over a wide range of angle of attack and at two different velocities.
Particular attention was devoted to the lift and pitching moment behavior
at low and negative angles of attack because of the potential loss of
longitudinal stability of flexible wing gliders in this regime. The
test results were used to estimate the performance and longitudinal con-
trol characteristics of the gliders.

INTRODUCTION

The flexible wing ultralight glider has evolved rapidly within the last
several years, and now bears little resemblance to the original parawing
configuration developed by NASA. This evolution has been characterised
mainly by cut and try flight testing rather than the application of
analytical design techniques or conventional wind tunnel testing. While
the evolutionary mode of development has yielded relatively advanced
configurations, little precise information exists about the aerodynamic
characteristics of these gliders. Such information, preferably obtained
from careful full scale wind tunnel testing, would be useful for numerous
purposes. For example virtually no accurate information on maximum lift
coefficients or maximum lift-to-drag ratio exists. Measuring these charac-
teristics would be helpful in guiding future design refinements to enhance
performance. Accurate test data on pitching moment characteristics is
needed because even the basic static longitudinal stability and control
characteristics of flexible wing gliders depend on complex aeroelastic

behavior of the flexible sail and frame. In certain unusual flight conditions, a loss of longitudinal stability may occur, which is believed to have contributed to in-flight structural failures. The identification and solution of such problems is hindered by a lack of accurate aerodynamic pitching moment data for various glider configurations.

The present experiments were undertaken to provide a limited amount of test data on the lift, drag, and pitching moment characteristics of four typical flexible wing ultralight gliders. The tests were carried out using conventional equipment and instrumentation in the settling chamber of a small scale subsonic wind tunnel. Because of certain limitations of the facility and equipment, the range and accuracy of the results are less than might be desirable; nevertheless useful information is provided, and the feasibility of the present techniques was evaluated.

NOTATION

A_p	pilot flat plate drag area, ft^2
b	wing span, ft
$\bar{c}$	average chord, S/b, ft
C_L	lift coefficient, L/qS
C_D	drag coefficient, D/qS
C_{D_p}	pilot drag coefficient, A_p/S
C_m	pitch moment coefficient, $M/qS\bar{c}$
D	aerodynamic drag, lb
F_c	pilot control force, pull force positive, lb
L	aerodynamic lift, lb
ℓ	distance between pilot tether point and application point of F_c, ft
L/D	lift-to-drag ratio, including pilot drag $C_L/(C_D+C_{D_p})$
M	aerodynamic pitch moment about pilot tether point, positive nose up, ft-lb
q	dynamic pressure, $1/2\rho V^2$, lb/ft^2
R/S	rate of sink, $V \sin(\tan^{-1}D/L)$, ft/min

S	projected wing area, ft^2
V	velocity, ft/sec(or mph)
W_g	glider empty weight, lb
W_p	pilot weight, lb
W/S	wing loading, lb/ft^2
α	angle of attack, measured with respect to keel chord line, degrees
ρ	air density, $slugs/ft^3$

TEST APPARATUS

The gliders were tested in the 30- X 33-ft settling chamber of a 7- X 10-ft subsonic wind tunnel. Maximum velocity in the settling chamber is approximately 18 mph, but the test velocity was limited to 15.8 mph due to strain gage balance load limits. The gliders were mounted 10 ft above the floor of the settling chamber at the top of the main support strut shown in Figure 1. The gliders were mounted directly to a T-bar adapter frame which clamped to the gliders' triangular control bar. The upper end of the T-bar frame was attached directly to the forward end of a six-component strain gage balance which in turn was mounted on top of the main support strut. Details of the mounting system are shown in Figure 2. With this system, the balance moment center was located very close to the pilot tether point of the glider which was taken to be the aerodynamic force and moment reference center of the glider. The balance mount could be rotated by remote control to vary the glider angle of attack. No provision was made for simulating pilot drag effects. Drag measurements were made of the gliders alone except for the small additional contribution of the T-bar adapter frame drag.

The strain gage balance had a normal force capacity of 1400 lb, an axial force capacity of 280-lb and a rolling moment capacity of 1200-in-lb. Tunnel turbulence and small lateral asymmetries of the gliders produced high rolling moments relative to the balance roll moment capacity and thus limited the maximum test velocities. Because of the low aerodynamic drag at these velocities, and the relatively high balance axial force capacity, the accuracy of the drag measurements was moderately low. The compromise between balance accuracy and capacity resulted from testing very large span models at low velocities using a strain gage balance designed for small, high speed models. The aerodynamic lift and pitch moment were measured with acceptable accuracy.

The four gliders tested were typical of intermediate to moderately high performance flexible wing ultralight gliders. Wing spans ranging from 25 to 30 ft were chosen in order to minimize tunnel wall interference effects as much as possible in the 33-ft wide settling chamber test section. Glider geometric parameters are listed in Table 1 and the wing planforms are illustrated in Figure 3. The Flexi 2 and Cirrus 3 are intermediate performance gliders having moderate billow sails. The Astro and Mirage are moderate to high performance gliders with higher aspect ratio and low to zero billow sails. Both have semi-floating tip ribs that limit the minimum wing tip washout in order to prevent the development of large negative aerodynamic pitching moments at low or negative angles of attack. The Astro was tested both with and without the floating ribs installed to assess their effectiveness. The Mirage was equipped with stiff cambered aluminum airfoil ribs; the other three gliders used flexible plastic or fiberglass battens. Each of the gliders is shown mounted in the wind tunnel settling chamber in Figure 4.

The test procedures were straightforward. After making wind off measurements to obtain model weight tares as a function of angle of attack, the gliders were tested at two different tunnel velocities. The angle of attack was varied while the tunnel velocity was held constant. This produced a variable sail loading which resulted in different wing aeroelastic deformations than would occur in normal 1g flight. This loading effect will be discussed in more detail below. Each glider's test angle of attack range was constrained by balance roll moment limits. At the higher tunnel velocity a smaller range of angle of attack was tested than at the lower velocity.

The data was processed as follows. For each test point, ten sets of balance data were taken and averaged to minimize the effects of tunnel turbulence and scatter in the balance readings. Wind tunnel wall corrections were made to correct the geometric angle of attack for the induced upwash of the tunnel boundaries. At high lift the induced angle was about 2.5°. The model forces were resolved into lift and drag components in the corrected (for induced angle) wind axis system. No other tunnel blockage, bouyancy, or support interference corrections were made. The data was reduced to coefficient form based on the projected wing area (not the flat sail pattern areas) and the wing average chord (wing area divided by wing span). The angle of attack was taken to be the keel angle of attack. The moment center for pitching moments was taken as the pilot tether point. As noted above, the balance accuracy was limited by a combination of low aerodynamic force levels and high balance force capacities. While it is difficult to determine precise accuracies, the following are believed to be reasonable estimates of the accuracy of the data presented below: $C_L = \pm .05$, $C_D = \pm .03$, and $C_m = \pm .02$.

EFFECT OF TEST LIMITATIONS

Before presenting the test results it will be useful to discuss the significance of the two important limitations of the tunnel facility used for the present tests. First, it must be emphasized that the wind tunnel

test results were obtained under conditions different from those experienced by a glider in steady state flight (unaccelerated 1g flight). Aside from measurement errors and wind tunnel wall effects, testing at constant velocity (as in the present tests) generates aeroelastic effects that alter the measured results from results that would be obtained by an exact duplication of actual flight conditions. Keeping the velocity constant as the glider angle of attack is varied changes the total aerodynamic sail loading at each angle of attack. In steady 1g flight the angle of attack and velocity automatically change in such a way that the resultant aerodynamic force remains constant and equal to the total weight of the glider and pilot. Therefore, for a given angle of attack the tunnel test condition and the actual flight condition would not in general produce the same level of aerodynamic load acting on the sail. Since different loads would generate different aeroelastic deflections of the glider sail and frame, the aerodynamic coefficient data, particularly the pitch moment coefficient, would be different for the two conditionss. The sail loading effect is also expected to be more pronounced for more flexible structures and higher billow sails.

Of course it would be possible to duplicate the aeroelastic effects of steady flight conditions in the wind tunnel by appropriately varying the tunnel velocity as a funtion of angle of attack to maintain a constant aerodynamic loading, or vary the angle of attack for a large number of test velocities and crossplot the results for a constant load condition. This procedure was not feasible for the present testing because tunnel and balance limitations did not permit testing at a sufficiently high range of velocities. However the results that are presented for two different test velocities do show the variations that would be anticipated from changes in sail loading.

Because of the relatively small test section size compared to the glider wing spans, the data is significantly influenced by induced flow effects of the tunnel floor and wall boundaries. As noted above, a correction is made for the induced angle of attack which accounts for the first order effects of the tunnel walls on wing angle of attack and the wing induced drag. It does not however, account for the effect of altering the wing span load distribution and the resultant secondary effect on induced drag. For the larger span gliders tested, this wall effect increases the loading at the wing tips and would be expected to slightly reduce the measured drag by reducing the induced drag. This is due to the fact that flexible wing gliders generally exhibit substantial tip washout which degrades the span load distribution by reducing the local section angle of attack at the tips. The effect of wall interference is to make up part of the lift lost to washout. Another effect of increasing the wing tip loading due to wall effects would be to promote tip stalling compared to free air testing. The effective reduction in washout due to wall induced effects at high lift conditions was not excessive however, being on the order of 1° to 2°.

RESULTS

Two sets of results are presented. First the lift, drag, and pitch moment coefficients as a function of angle of attack for two test vel-

ocities are presented for the five different glider configurations tested (Flexi 2, Cirrus 3, Mirage, Astro, and modified Astro without floating tip ribs). The second set of results gives the longitudinal control and performance characteristics derived from the basic wind tunnel test data. For these results, an arbitrary pilot drag increment is added to the drag data of each glider.

Figures 5 through 9 show C_L, C_D, and C_m vs α for all of the glider configurations. The data points are labelled according to the measured test dynamic pressure, q=0.25, 0.38, and 0.64 lb/ft^2. For standard sea level density the corresponding test velocities for these three dynamic pressures are V=9.9, 12.2, and 15.8 mph respectively. Generally the effects of increasing dynamic pressure are to increase sail loading, increase washout, and thereby reduce the lift coefficient slightly and increase the pitch moment. Figures 10-12 compare the faired lift, drag, and pitching moment curves of the five configurations. This comparison provides the most consise summary of the basic results. Generally the gliders can be divided into two relatively distinct categories, each having certain unique aerodynamic features. First are the low aspect ratio, moderate billow gliders, the Flexi 2 and the Cirrus 3. Second are the higher aspect ratio low billow gliders with the floating tip ribs, the Mirage and Astro.

Consider the lift curves in Figure 10. The low aspect ratio gliders exhibit a distinct zero slope nonlinearity in the region of zero lift due to sail luffing. With the sail loaded, the lift curves are quite linear, and no sign of stall is evident even at high angles of attack and relatively high lift coefficients (maximum angle of attack was limited by balance loads). The high aspect ratio gliders exhibit virtually no luffing behavior in the zero lift region, except for a mild curvature of the lift curves near zero lift. Stall begins at moderate angles of attack and maximum lift coefficients of about 1.4 are exhibited with very gentle stall behavior. The modified Astro develops more lift at low angles of attack than the standard Astro configuration due to reduced tip washout with the floating tips removed. If the wing were more highly loaded at low angles of attack, these differences would be much smaller.

The drag curve comparisons are given in Figure 11 and no major surprises are to be found. As indicated earlier the absolute accuracy of the drag curves is less than desired but the trends appear reasonable. The high aspect ratio configurations exhibit a rather abrupt increase in the slope of the drag curve between 10° to 12° angle of attack. Visual observations of wool tufts attached to the upper wing surface indicated that the drag rise point coincided with the onset of flow separation. The separation began at the wing tips and extended gradually inboard from the tips as the angle of attack increased. The wing root became stalled only at the highest angles of attack tested, approximately 30° to 35°.

The pitching moment curves in Figure 12 are particularly interesting. It is believed that the artificial loading conditions produced during the tunnel testing influenced both the absolute pitch moment levels as well as the slope of the pitch moment curves. Therefore only certain conclusions can be drawn. First consider the low aspect ratio gliders for

562

which the loading effects are believed most pronounced. In the normal angle of attack range the pitch moments are negative, i.e. there is no zero moment trim point. If results were available at higher velocities and the results were crossplotted for a constant loading conditions, it is believed that these curves would indicate trimmed ($C_m=0$) stable ($dC_m/d\alpha<0$) behavior at a reasonable angle of attack ($\alpha \simeq 15°$). As they stand the results show larger negative values and lower slopes than are consistent with observed control characteristics of these particular gliders. At negative angles of attack, the sails of the low aspect ratio gliders become unloaded, and collapse against the glider crossbar structure radically altering the wing camber and twist. The result is negative washout at the wingtips, and large effective camber near the root of the wing, both of which contribute to yield a large negative pitch moment. The practical significance of these results is that if transient negative angle of attack conditions were encountered in flight, a divergent pitch instability could possibly result.

The high aspect ratio, low billow glider configurations compared in Figure 12 exhibit quite different behavior although the sail loading effects still appear to be significant because of the inconsistency between the measured and observed flight trim characteristics. The most significant departure from the low aspect ratio gliders is that the Astro and Mirage exhibit a positive increment in pitch moment as the sail unloads in the zero lift region. It is interesting that this phenomenon manifests itself in the moment curve but not the lift curve. The increase in moment is believed due to the effective increase in washout (i.e. wing twist) as the inboard portion of the wing unloads and settles onto (trailing edge down) the wing cross spar. While the floating tip ribs of the Astro are effective in maintaining sufficient washout to produce positive pitch moments at low and negative angles of attack, the lower minimum angle of the Mirage floating tip rib was evidently insufficient to produce comparable results. Interestingly, while the modified Astro (tip rib removed) did exhibit much lower pitch moment at negative angles of attack compared to the standard Astro, it also exhibited a positive moment increment at the zero lift point. It was anticipated that this configuration would exhibit the opposite behavior, i.e. a negative pitch moment increment due to loss of washout at negative lift similar to the low aspect ratio gliders. A possible explanation of this behavior is that camber variations of the pre-tensioned, zero-billow sail counteracted the loss of washout at zero lift conditions.

To summarize the pitch moment results, the low billow, tip-rib-supported configurations exhibited more favorable pitch moment characteristics at negative angles of attack than did the lower aspect ratio, larger billow sail configurations.

Finally, the high aspect ratio configurations exhibited stable pitching moment changes at stall, i.e. an increased negative slope of the moment curve. (The low aspect ratio gliders' test angles of attack did not extend into the stall region.) This is somewhat surprising in view of the observed separation at the wing tips and the well known tendency of moderate and high aspect ratio swept wings to exhibit pitchup tendencies

563

at stall. It is possible that the high twist of the present flexible wing configurations helps to prevent such behavior.

The second set of results in Figures 13-17 was prepared to illustrate the applicability of the wind tunnel test data to performance and longitudinal control predictions and to indicate typical flight characteristics of the glider types tested. For these results, a nominal wing loading based on manufacturer specifications was assigned to each glider and an incremental pilot drag coefficient was also added to the drag coefficient test data. This drag was scaled to pilot size which was related to pilot weight. The pilot weight was determined by the individual glider empty weight and the assigned wing loadings. The pilot drag to weight relationship is given by the following formula

$$C_{D_p} = \frac{A_p}{S} = \frac{2.5}{S} \left(\frac{W_p}{160}\right)^{2/3}$$

This is based on assuming a flat plate drag area of 2.5 ft^2 for a 160-lb pilot and relating pilot size to weight by a square-cube relation. Table 2 gives the relevant parameters for pilot drag calculations for each glider. The glider airspeed, sink rate, and control forces were calculated for standard sea level conditions $\rho = 2.378 \times 10^{-3}$ slug/ft^3 using appropriate relations. The control forces were determined from the following relation

$$F_c = C_m \, q \, S \, \bar{c} \, / \, \ell$$

where ℓ was assumed to be 5.0 ft for all the gliders. This relation assumes that the pitch moment coefficient is taken about the pilot tether point and that the pilot control force is applied to the control bar a distance ℓ from the tether point.

As discussed above, the effects of the test loading conditions are not believed very significant for lift and drag coefficient data and thus the L/D and sink rate performance are believed to be reasonably valid in this respect. The low accuracy of the drag coefficient data does limit the absolute accuracy of the performance data; therefore, valid comparisons between the different glider types cannot be made. Again, the variations in L/D and R/S with airspeed are more accurate. Finally because the test loading conditions have a substantial effect on the pitch moment coefficient results, the control force variations with velocity are not fully representative of actual flight conditions.

Figures 13-17 indicate that maximum L/D values occur only for a relatively narrow velocity range; the minimum sink rate is not quite so sensitive to velocity. For the Astro and Mirage, the minimum sink rate condition coincides with the point where wool tuft observations indicated the onset of flow separation. The effects of test velocity are relatively small for L/D and sink rate, but are more substantial for the longitudinal control force. Even though the pitch moment coefficient data was generally negative, the resulting control forces are not excessive. A positive

564

slope of the control force versus velocity curve indicates a statically stable configuration. Nearly all configurations show a very stable slope near the minimum flight speed. The Astro shows a reasonably well behaved control force variation that is stable at all velocities, trims to zero force (although at a rather unrealistic 53 mph) and exhibits a large increase in stability at stall. Finally, the high lift coefficients yield relatively low minimum velocities.

For comparison purposes, the faried L/D and sink rate curves are given in Figures 18 and 19.

CONCLUDING REMARKS

Testing of full scale flexible wing ultralight gliders in the settling chamber of a subsonic wind tunnel provided useful information about the glider aerodynamic characteristics. The limitation on maximum test velocity prevented full simulation of load conditions corresponding to normal flight. Two low aspect ratio moderate billow gliders exhibited sail luffing effects in the lift curves, increased negative pitching moment at negative angles of attack, and evidence of high maximum lift coefficients. The higher aspect ratio, low billow configuration lift curves showed only minor evidence of zero lift sail luffing; the pitch moment curves showed a positive moment increment as lift decreased below zero. The high aspect ratio configurations showed gradual lift and increasingly stable moment variations at stall although wool tuft flow visualization indicated flow separation commencing at the wing tips. The drag variation with angle of attack increased abruptly with the observed onset of flow separation. The effect of floating tip ribs was to substantially increase the wing pitching moment of the Astro at negative angles of attack. The Mirage floating tip ribs appeared to be less effective, presumably because of a lower minimum washout angle. Except for control force characteristics, performance estimates based on the test data appear consistent with typical operating experience.

TABLE 1 - GLIDER GEOMETRIC PROPERTIES

	Flexi 2	Cirrus 3	Mirage	Astro
Projected wing area, ft²	192.0	193.1	113.6	144.4
Wing span, ft	29.43	28.14	25.56	28.74
Nose angle, degrees	95	91	112	108
Leading edge sweep, degrees	42.5	44.5	34.0	36.0
Aspect ratio	4.50	4.09	5.77	5.70
Root chord, ft	15.04	12.83	7.58	9.23
Average chord, ft	6.53	6.87	4.44	5.02
Moment center, percent of root chord behind root chord leading edge	49.0	58.1	66.0	62.1
Vertical moment center, distance below bottom of keel tube, ft	0.47	0.58	0.47	0.50
Billow, per side, degrees	2.5	1.25	0.66	0.0
Number of battens or ribs per side	2	6	4	4
Floating tip rib minimum washout (estimated), degrees	----	----	8	16

TABLE 2 - PILOT DRAG DATA

Glider	W_g, lb	W/S lb/ft^2	W_p, lb	C_{D_p}
Flexi 2	41	1.0	151	.0125
Cirrus 3	39	1.05	164	.0131
Mirage	35	1.1	90	.0150
Astro	40	1.2	133	.0153
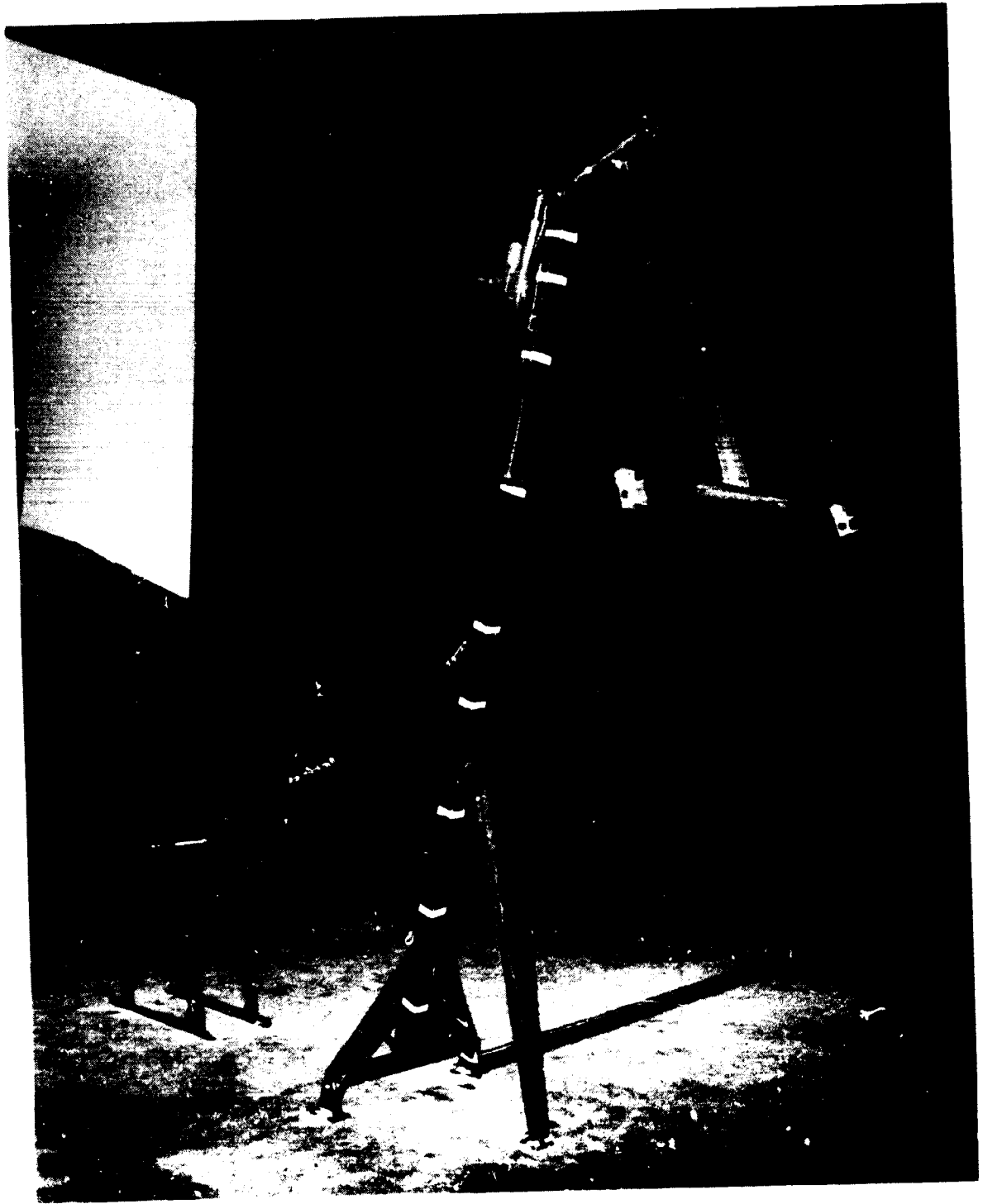
Figure 1 - Main support strut and T-bar adapter frame.
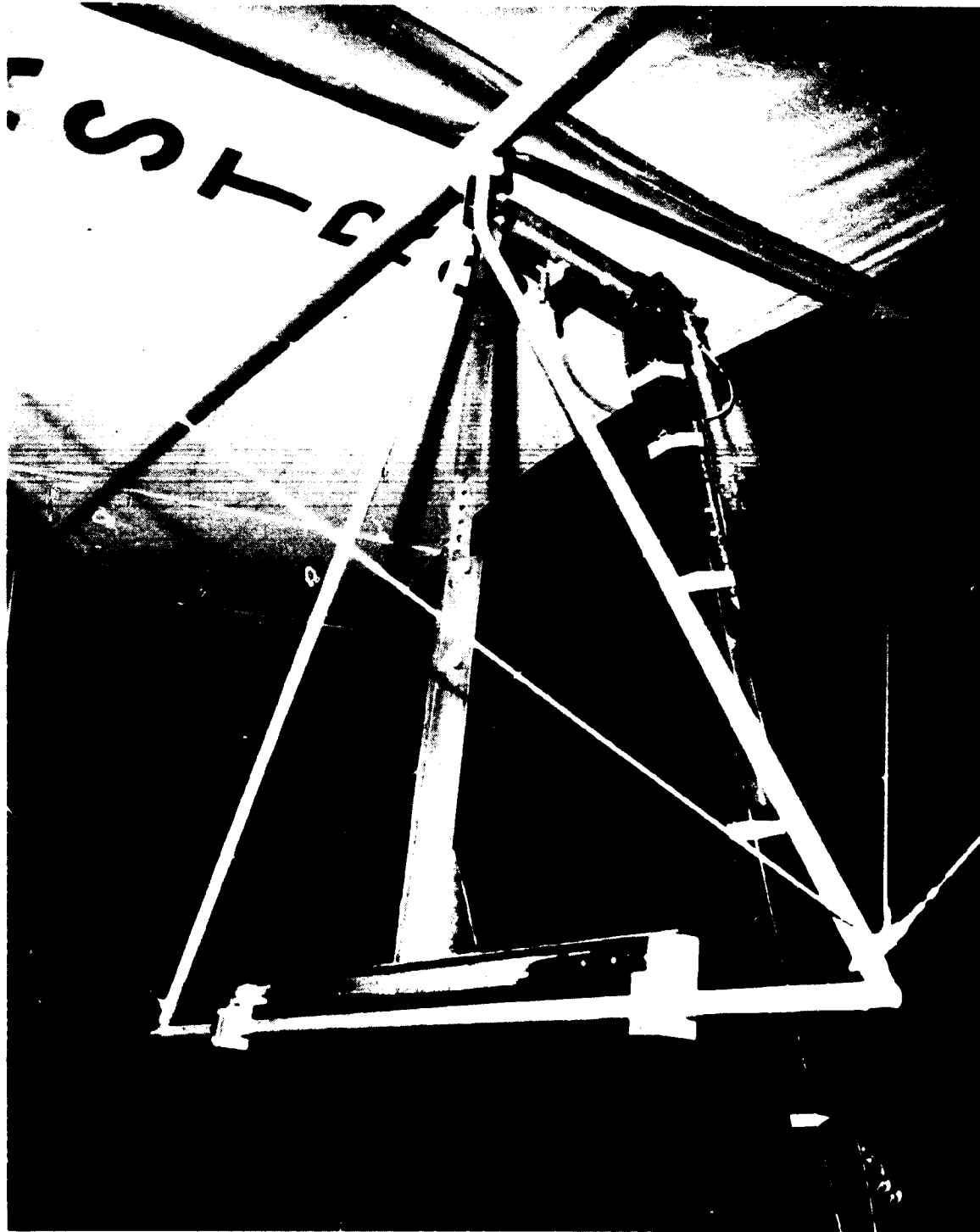
Figure 2 - Details of glider mounting on T-bar adapter frame.

MIRAGE

ASTRO
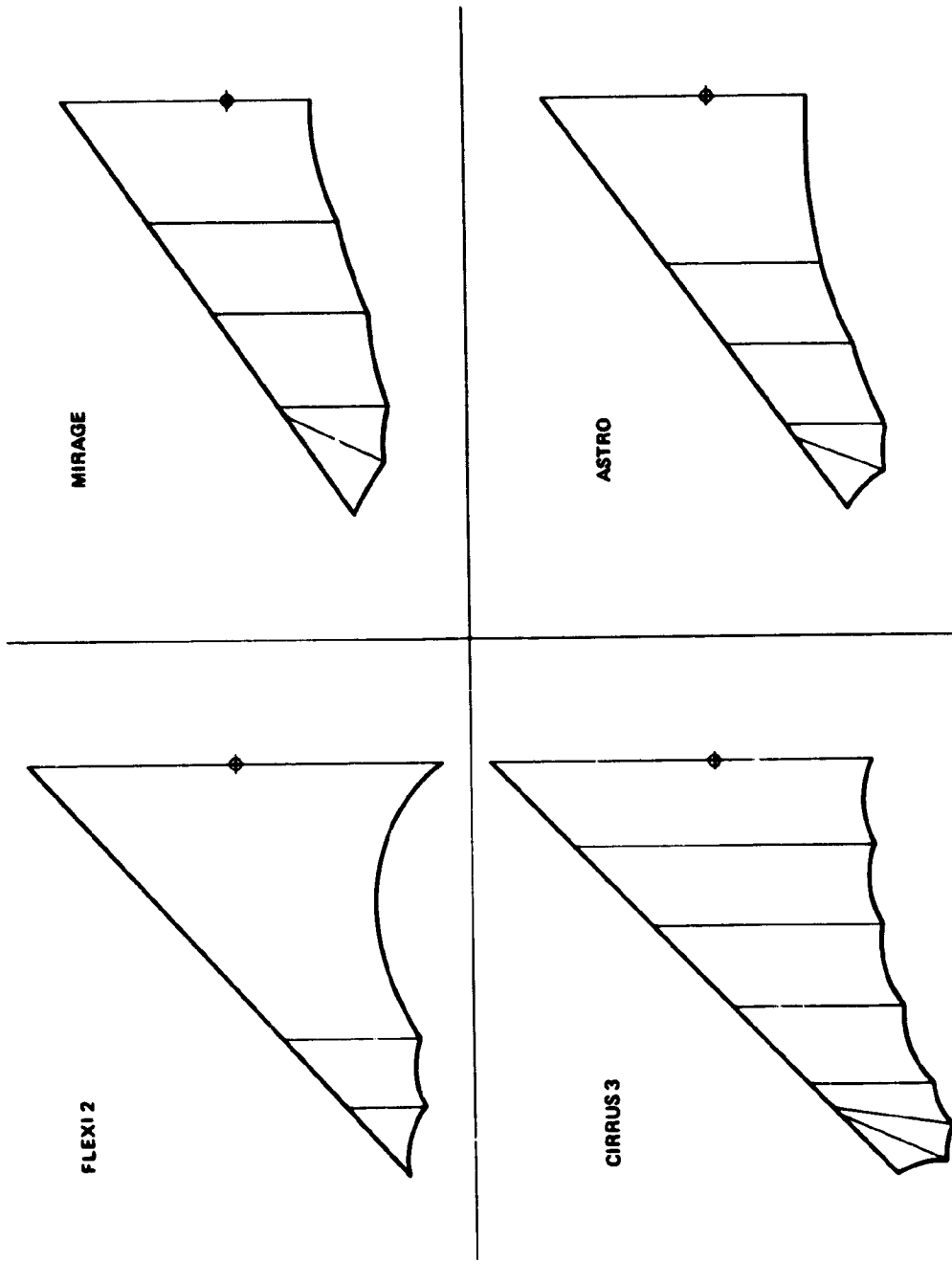
FLEXI 2

CIRRUS 3

Figure 3 - Glider wing planforms.
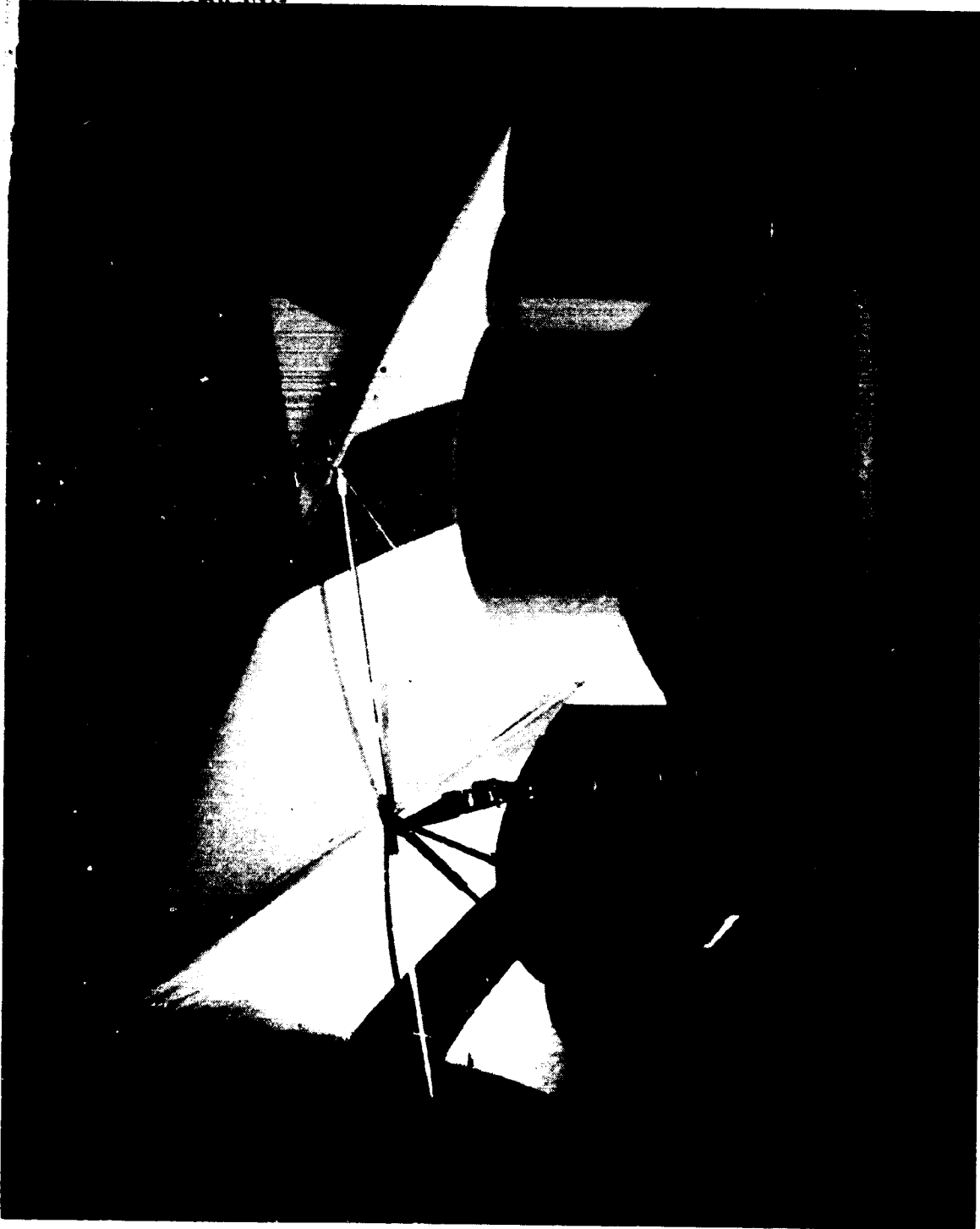
Figure 4a – Flexi 2.

Figure 4b – Cirrus 3.
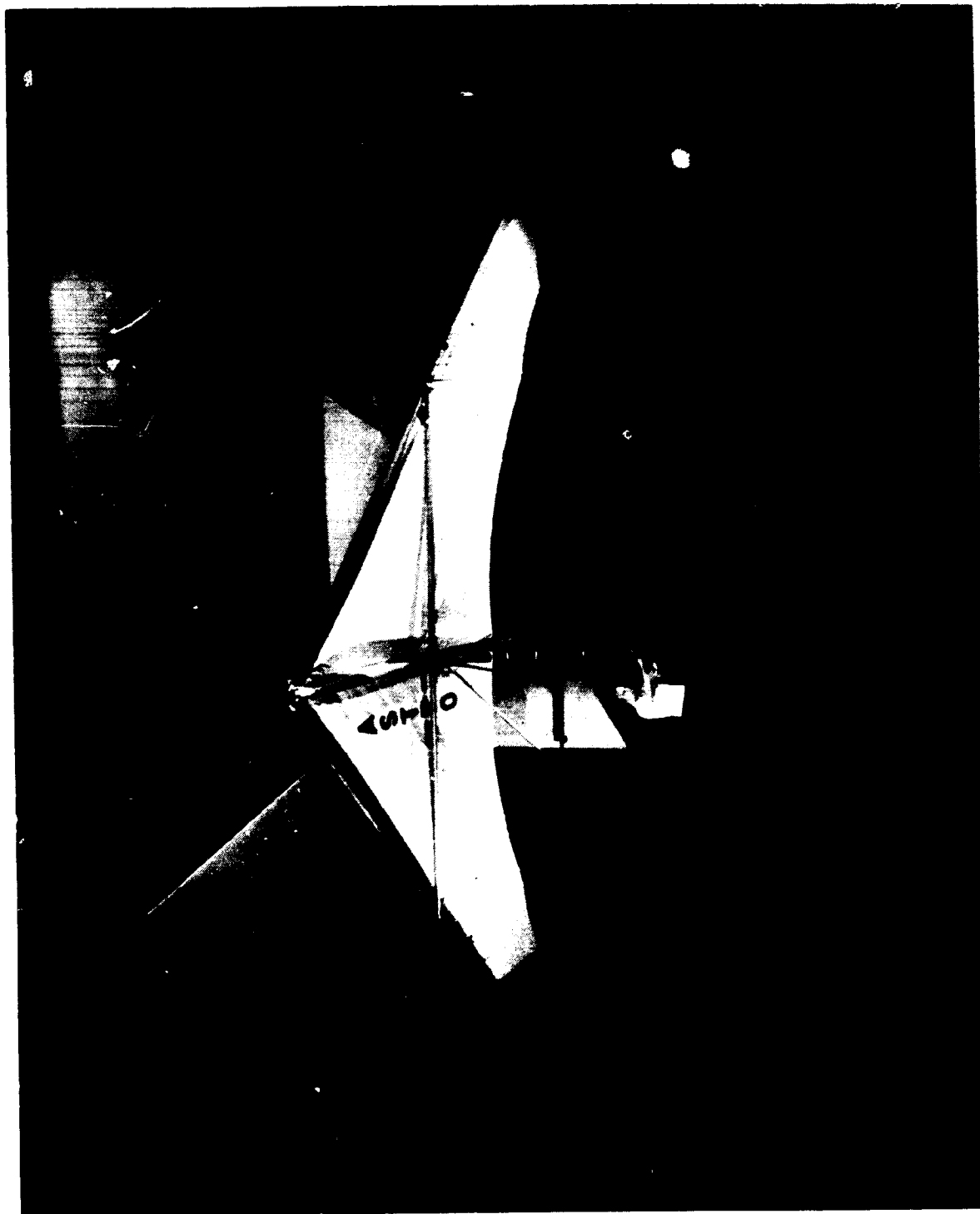
Figure 4c – Mirage.

Figure 4d – Astro.
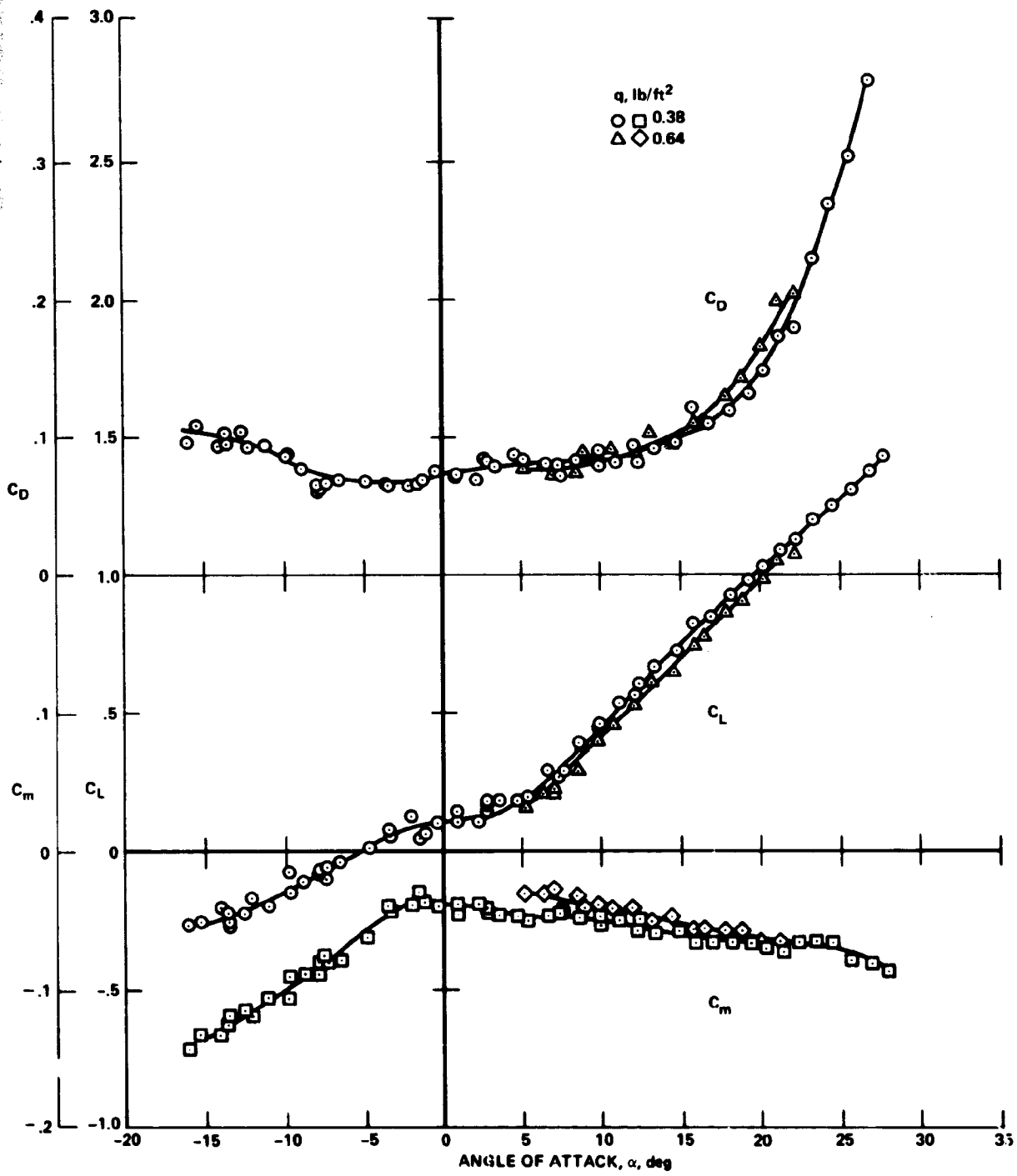
Figure 5 – Flexi 2 lift, drag, and pitch moment coefficient test data.
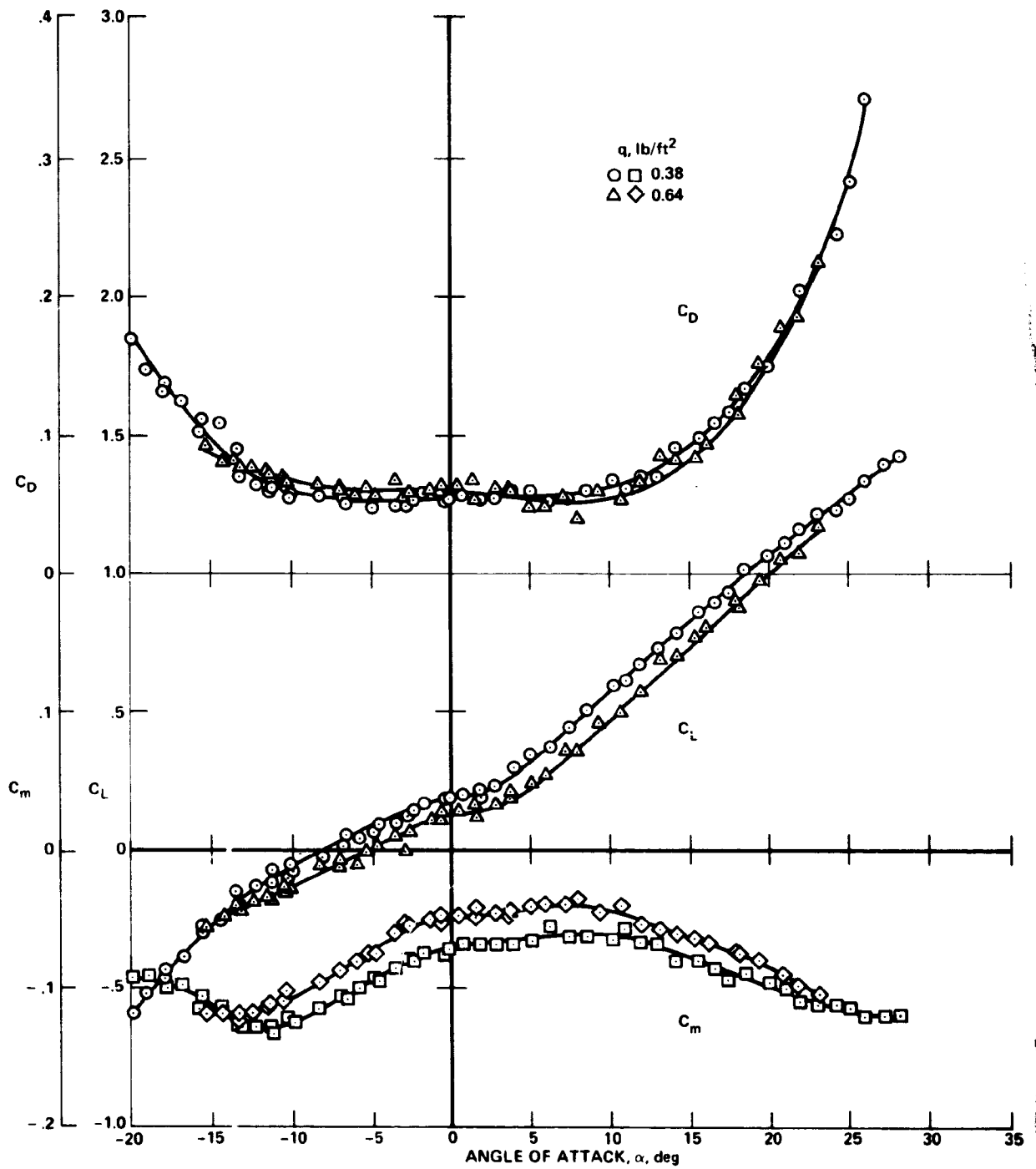
Figure 6 – Cirrus 3 lift, drag, and pitch moment coefficient test data.
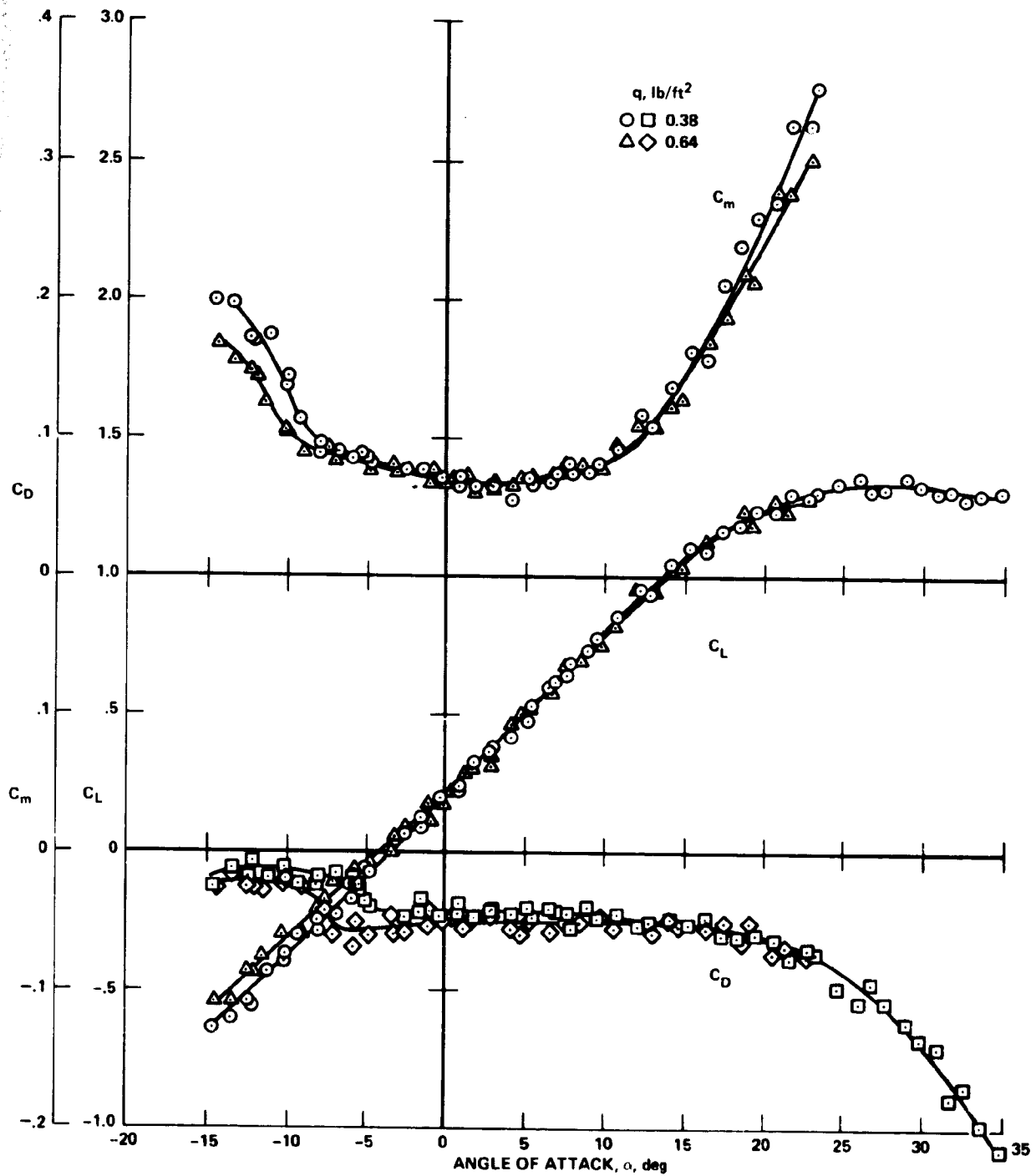
Figure 7 – Mirage lift, drag, and pitch moment coefficient test data.
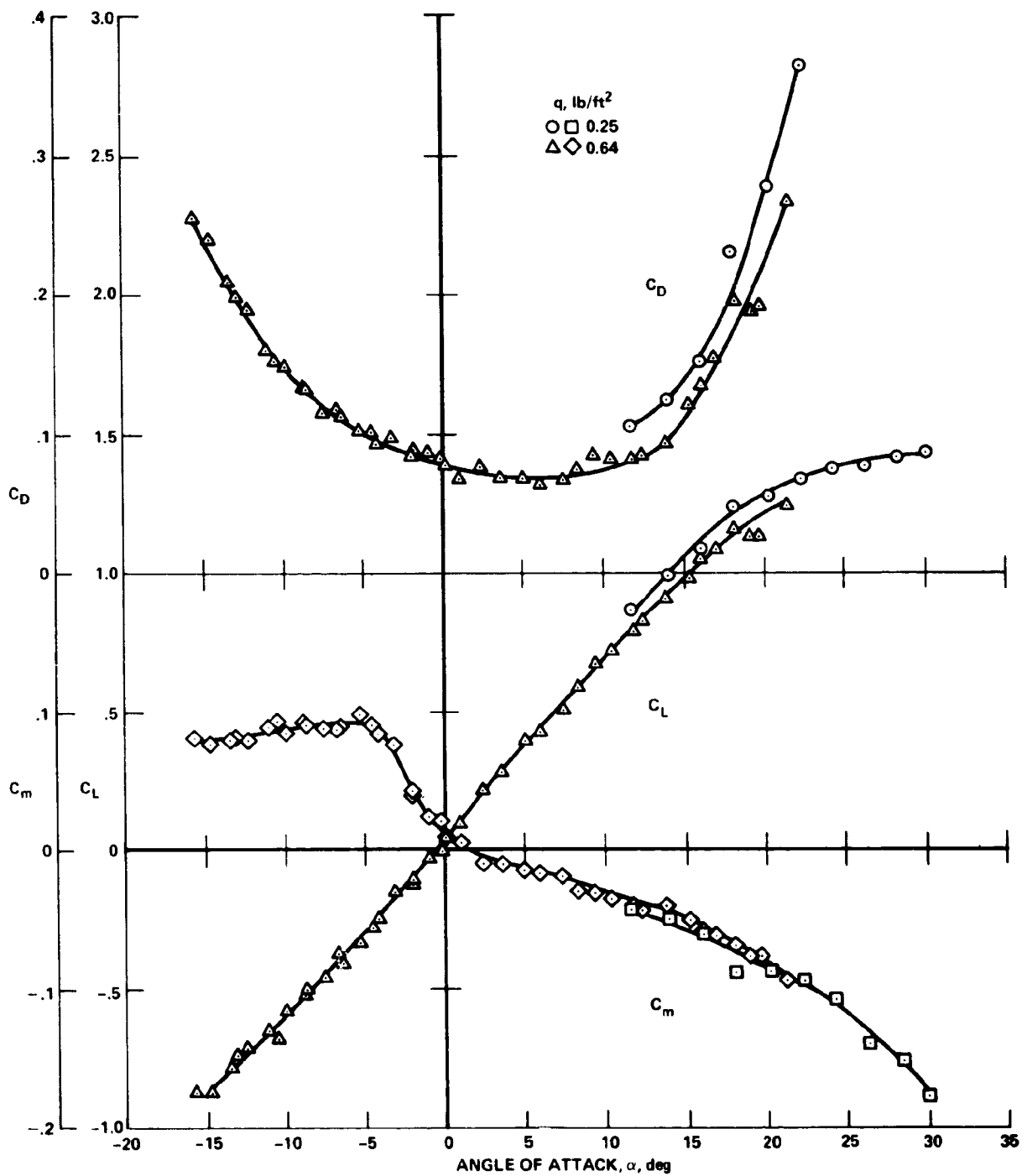
Figure 8 - Astro lift, drag, and pitch moment coefficient test data.
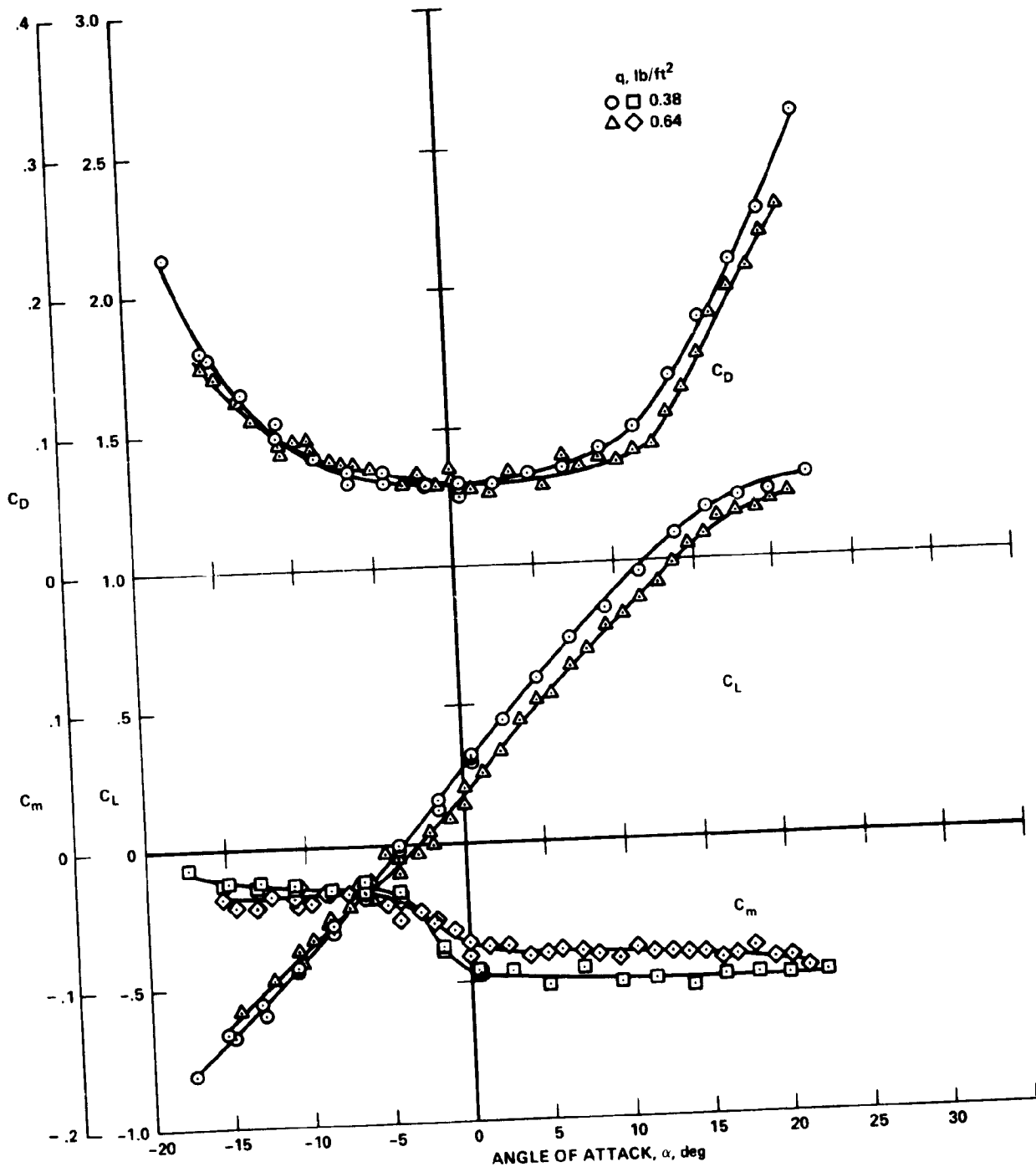
Figure 9 – Modified Astro (floating tip ribs removed) lift, drag, and pitch moment coefficient test data.
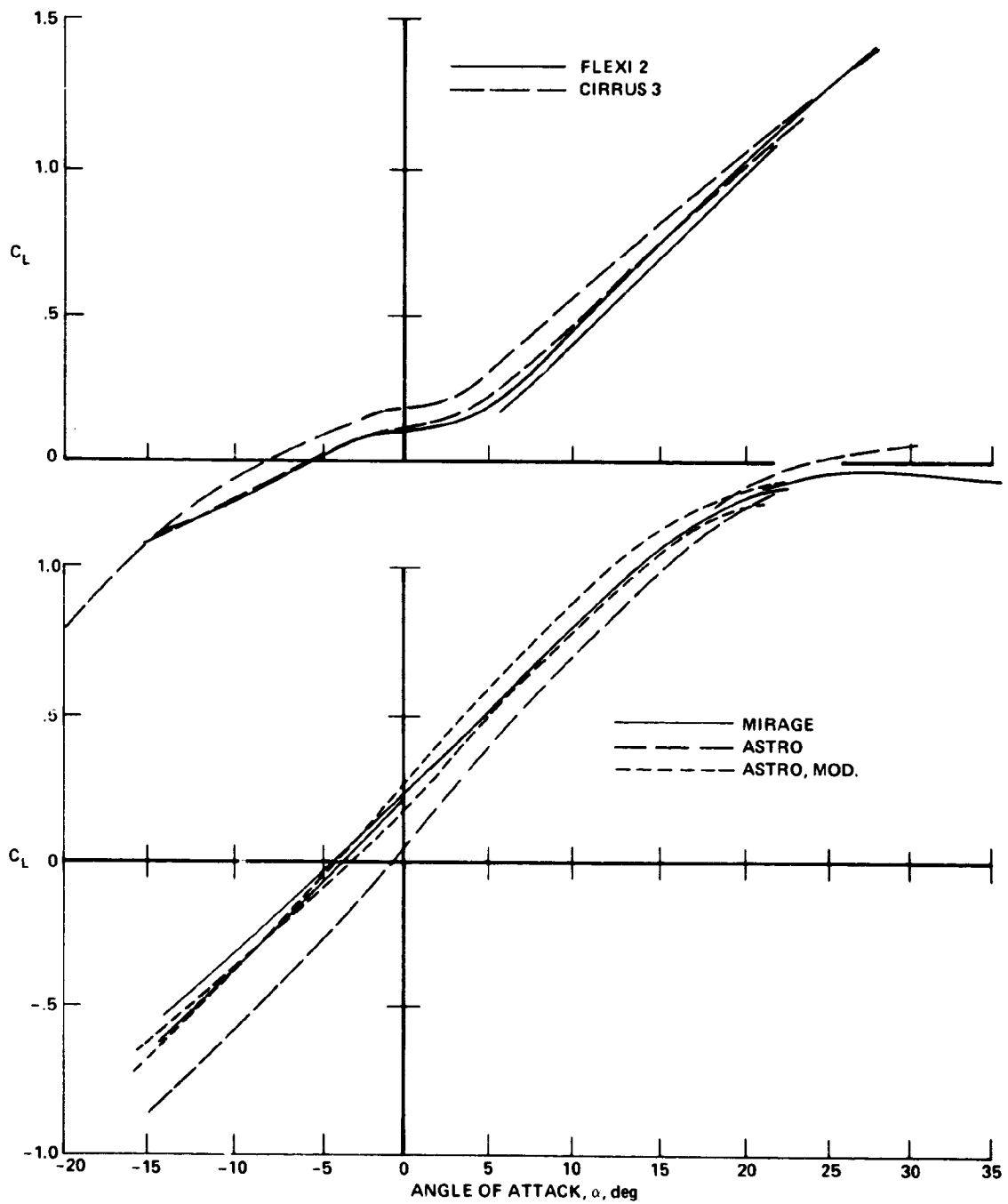
Figure 10 – Comparison of faired lift coefficient curves from Figures 5–9.
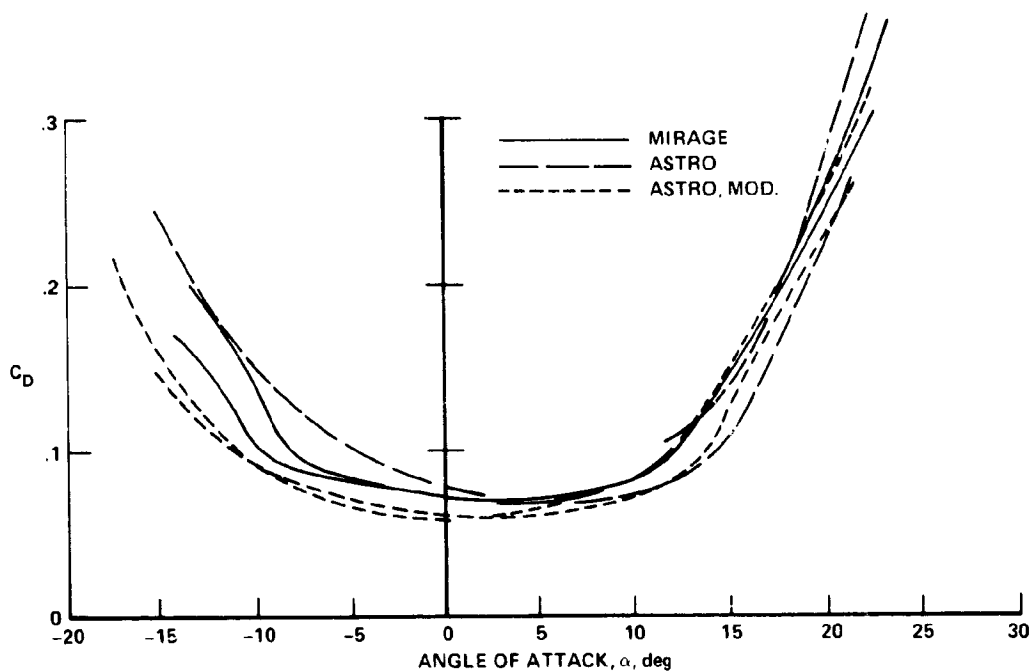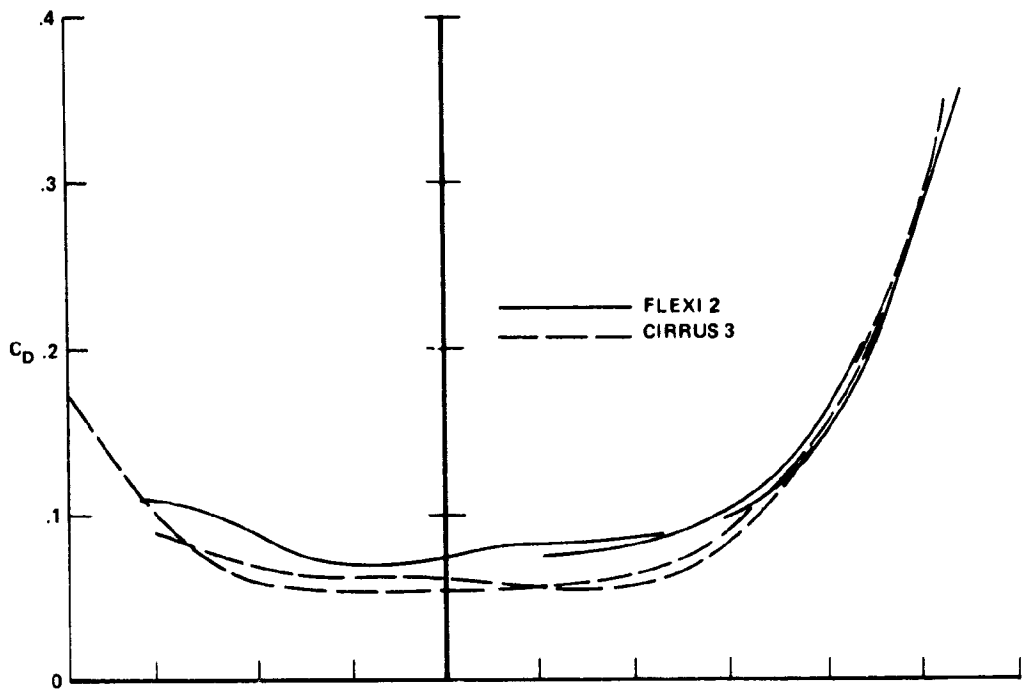
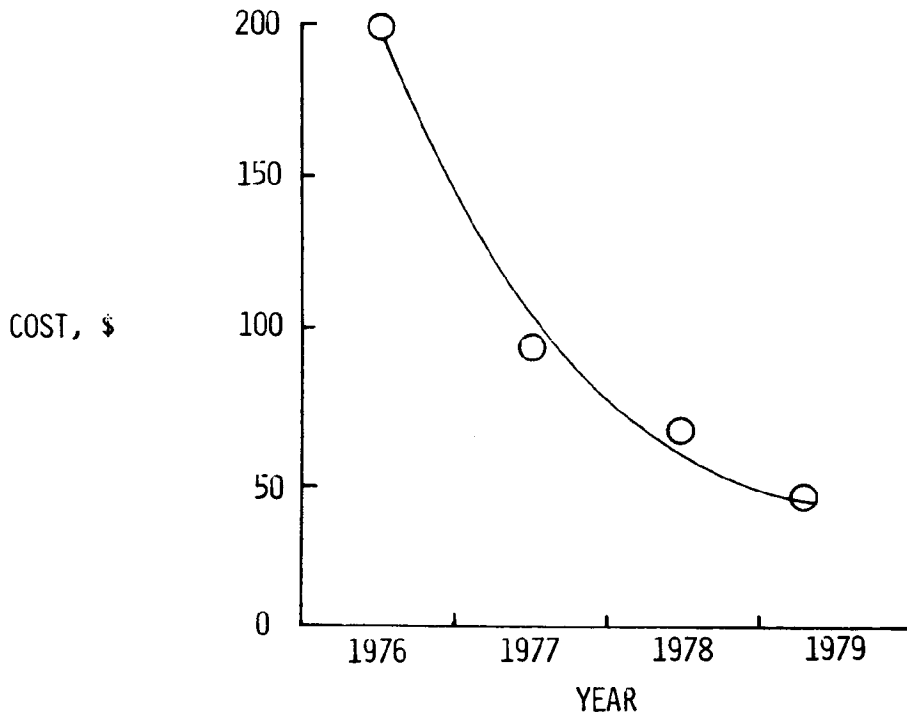Figure 11 - Comparison of faired drag coefficient curves from Figures 5-9.
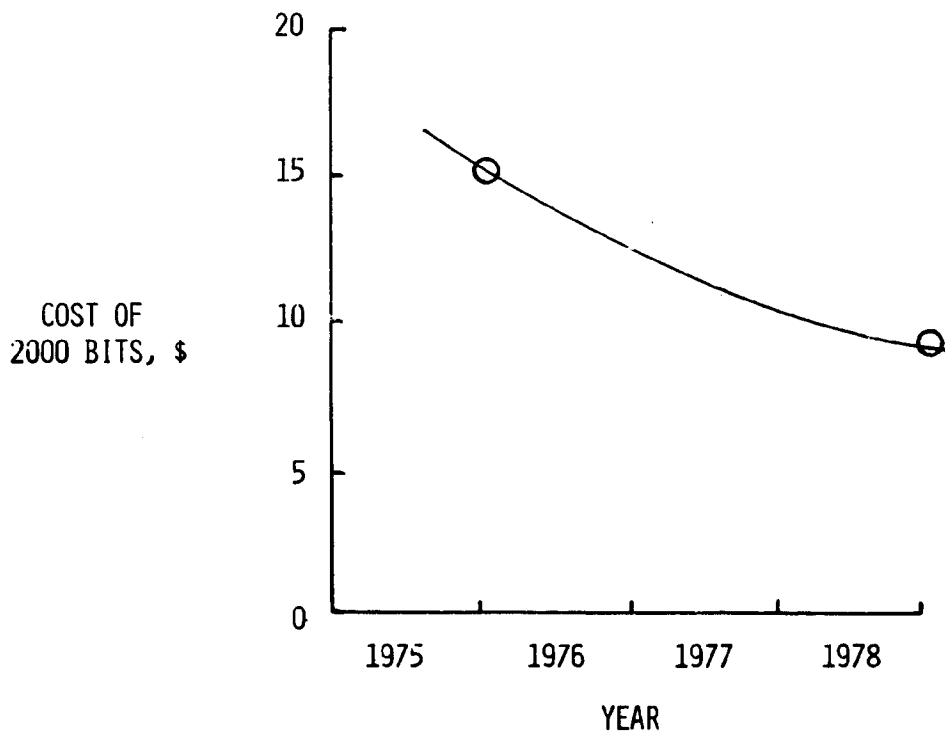
Figure 10.- Cost trend of typical 16-bit microprocessor.
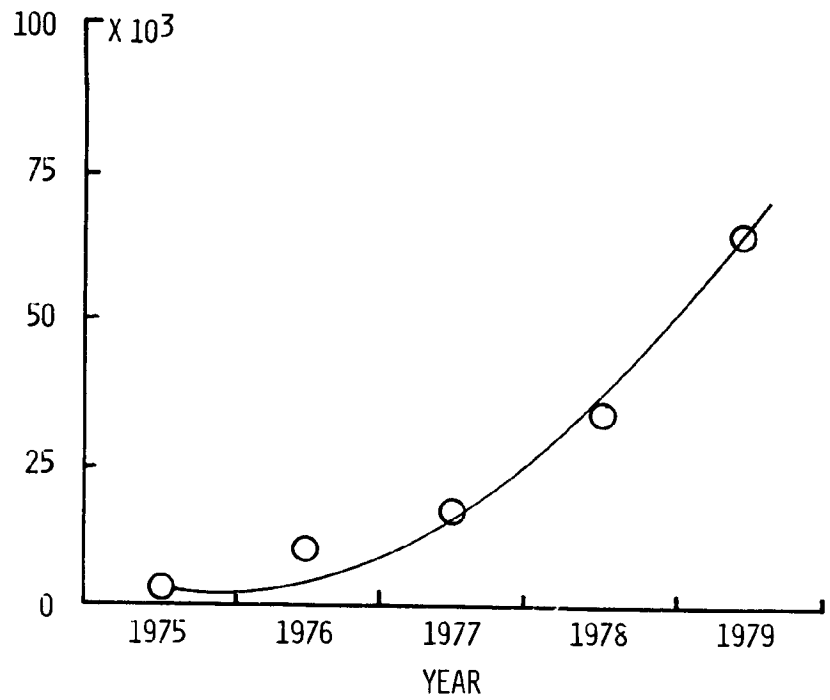

Figure 11.- Cost trend of RAM memory.

C-4

Figure 12.- Trend of amount of memory per package.